A Novel Intercarrier Interference Cancellation for MIMO-OFDM Systems

Aurupong Yiwleak[1] and **Chaiyod Pirak**[2], Non-members

ABSTRACT

The main impairment of an orthogonal frequency division multiplexing (OFDM) systems is an intercarrier interference (ICI) effect caused by a frequency offset. A zero-padded technique designed for a conjugate cancellation scheme in MIMO-OFDM systems for ICI cancellation is proposed by padding zero between two consecutive symbols over a space-frequency domain. At the receiver, the ICI cancellation and space-frequency diversity combining techniques are proposed. In this paper, a performance analysis is investigated and analyzed. In comparison with the conventional complex conjugate scheme, the outage probability expressions of the proposed system and the repetition-coded conjugate cancellation scheme are derived for quasi-static Rayleigh fading channels. Simulation results show the close agreement with those obtained by theoretical analysis, which could be used to estimate the proposed system performance. Finally, simulation results in time-varying frequency-selective fading channels, a bit error rate (BER) performance of the proposed system is significantly improved over both the ordinary zero-padded MIMO-OFDM systems and the repetition-coded conjugate cancellation scheme when the frequency offset is not greater than 10% of subcarrier spacing. Furthermore, the proposed system is shown to be able to attain significant diversity gain.

Keywords: Frequency Offset, Intercarrier Interference (ICI), MIMO, OFDM, Outage Probability

1. INTRODUCTION

Multiple-input and multiple-output (MIMO) is a widely adopted technique in modern wireless communication systems because it can be used to improve diversity gain or to increase multiplexing gain [1]. When the multiple transmit or receive antennas are equipped with sufficient spacing, the channel impulse response between antennas fades independently, which in turn yields a space diversity [2]. The probability that all signals are in deep fade simultaneously is significantly reduced. The orthogonal frequency division multiplexing (OFDM) is another useful technique due to its high spectral efficiency and robustness to multipath fading channels. In frequency-selective fading channels, using this technique in MIMO systems could yield a diversity gain across space, time, and frequency domains. By allowing spectral overlapping of subcarriers in OFDM, it is sensitive to frequency offset, which is caused by a Doppler shift as well as a carrier frequency synchronization error. In frequency offset situations, the orthogonality among subcarriers may be destroyed, and thus can introduce intercarrier interference (ICI).

There are four techniques for ICI cancellation which have been proposed, including frequency-domain equalization [3], time-domain windowing [4], ICI self-cancellation [5-9] and two-path conjugate cancellation [10,11,12]. A conjugate cancellation was proposed [11], in which the first path represents the ordinary OFDM signal and the second path is the conjugate copy of the first path. In [12], the authors proposed a phase rotation for conjugate cancellation technique that can achieve a better performance in high frequency offset situations with the need of frequency offset estimation. Although most of these techniques have been proposed for single-input and single-output (SISO), the authors in [13] introduced the ICI self-cancellation scheme into MIMO-OFDM systems. However, the authors in [13] mainly focused on the space-frequency-coding design rather than ICI mitigation. The authors in [14] proposed ICI self-cancellation for Alamouti Coding in cooperative systems, in which the channel impulse response is restricted to real values. The authors in [15] and [16] proposed the zero padding technique for MIMO-OFDM systems by using time-domain complex-conjugate cancellation and frequency-domain self-cancellation schemes, respectively, which can enhance the diversity gain and support the complex-valued channels. However, there is a lack of thorough study of a complex-conjugate cancellation designed for multiple-antenna systems and the performance analysis of such system. The purposes of this paper are to investigate and analyze the performance of the zero-padded complex conjugate cancellation scheme for MIMO-OFDM systems. In comparison with the conventional system, the proposed system is compared with a repetition-coded complex-conjugate cancellation scheme. The main

Manuscript received on February 6, 2015 ; revised on September 2, 2015.

Final manuscript received on September 28, 2015.

[1,2] The authors are with Sirindhorn International Thai-German Graduate School of Engineering (TGGS), King Mongkut's University of Technology North Bangkok, Bangkok, Thailand, E-mail: aurupong.y@hotmail.com and chaiyod.p.ce@tggs-bangkok.org

contributions of this paper are as follows.

⟨*i*⟩ The proposed zero-padded complex conjugate cancellation in MIMO-OFDM systems can enhance the diversity gain over both the ordinary zero-padded systems without conjugate cancellation scheme and the conventional repetition-coded complex conjugate cancellation scheme, when the frequency offset is small.

⟨*ii*⟩ The outage probability has been derived for both the proposed system and the repetition-coded complex-conjugate cancellation scheme in Rayleigh quasi-static fading channels. The theoretical results for both of them are closed to their simulation results, which could confirm the validity of the theoretical analysis.

The rest of this paper is organized as follows. In Section 2, the mathematical models of OFDM systems with frequency offset and the conjugate cancellation scheme in [11] are described. In Section 3, the proposed zero-padded conjugate cancellation scheme in MIMO-OFDM system is presented. In Section 4, the performance analysis is investigated, and compared with the conventional scheme. In Section 5, the simulation results are presented, and the conclusions are given in Section 6.

2. OFDM SYSTEM MODEL WITH FREQUENCY OFFSET

2.1 OFDM System Model

The output complex baseband signal of the IFFT at the transmitter can be expressed as,

$$x_n = \frac{1}{\sqrt{N}} \sum_{l=0}^{N-1} X_l e^{j\frac{2\pi}{N}nl}, \quad n = 0, \ldots, N-1, \quad (1)$$

where N is the total number of subcarriers and X_l $(l = 0, ..., N-1)$ is the modulated symbols on the l^{th} subcarrier. At the receiver, the time-domain received signal is suffered from the frequency offset and an additive white Gaussian noise (AWGN), which can be described by [15]

$$y_n = (\sqrt{P_0}x_n \otimes h_n)e^{j\frac{2\pi}{N}n\Delta fT} + z_n, \quad (2)$$

where P_0 and h_n denote the transmit power and the channel impulse response, respectively; $e^{j\frac{2\pi}{N}n\Delta fT}$ denotes the corresponding frequency offset at the sampling instants with the frequency offset to subcarrier spacing ratio denoted as ΔfT, and z_n, modelled as zero-mean, complex Gaussian random variables with variance N_0, denotes the additive white Gaussian noise. Moreover, $\otimes$ denotes the circular convolution. In this paper, the authors fairly assume that a cyclic prefix is inserted at the transmitter and removed out at the receiver. Then, the frequency domain signal on the k^{th} receiving subcarrier at the output of the FFT, which is $Y_k = \frac{1}{\sqrt{N}} \sum_{n=0}^{N-1} y_n e^{-j\frac{2\pi}{N}nk}, k = 0, ..., N-1$, becomes,

$$\begin{aligned} Y_k &= \sum_{l=0}^{N-1} \sqrt{P_0} X_l H_l U_{l-k} + Z_k, \quad k = 0, \ldots, N-1, \\ &= \sqrt{P_0} X_k H_k U_0 + \sum_{l=0, l\neq k}^{N-1} \sqrt{P_0} X_l H_l U_{l-k} + Z_k. \end{aligned} \quad (3)$$

In (3), the first term is a desired transmitted data symbol, and the second term is the ICI term generated by other subcarriers. Note that H_k and Z_k denote the frequency-domain channel impulse response and the frequency domain of z_n, respectively. The U_{l-k} is the coefficient of FFT(IFFT), which can be expressed by

$$U_{l-k} = \frac{1}{N} \sum_{n=0}^{N-1} e^{j\frac{2\pi}{N}n(l-k+\Delta fT)}. \quad (4)$$

Note that U_{l-k} is a complex weighting function of the transmitted data symbols in the frequency domain.

2.2 Conjugate Cancellation Scheme and Its Property

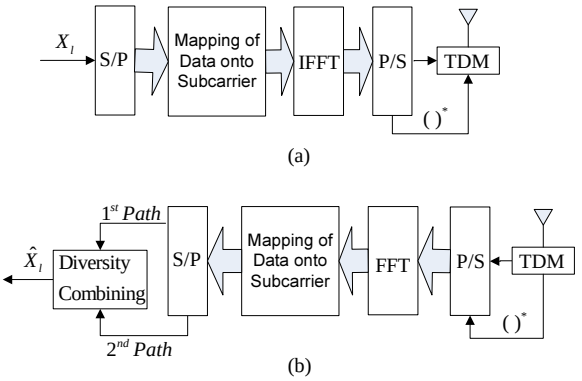

Fig.1: *Structure of a complex-conjugate scheme, (a) Transmitter, (b) Receiver*

In this subsection, the authors present a complex-conjugate cancellation technique as shown in Figure 1 [11]. The conjugate cancellation scheme transmits a complex-conjugate copy of the primary OFDM symbol in the second time interval, which provides opposite polarities of weighting coefficient at the zero crossing point. At the receiver, the combined received signal of both transmission intervals is the desired detected symbol. Assuming that the received signal in both intervals can be combined coherently without interfering with each other by using a time division multiplexing (TDM). The frequency offset is assumed to be fixed over the two-path time interval. The re-

ceived signal of the complex-conjugate path is given by [15]

$$y_n^{'} = (\sqrt{P_0}x_n^* \otimes h_n^{'})e^{j\frac{2\pi}{N}n\Delta fT} + z_n^{'}, \quad (5)$$

and the output of the FFT in the frequency domain signal on the k^{th} receiving subcarrier of the complex-conjugate path is expressed as, $Y_k^{'} = \frac{1}{\sqrt{N}}\sum_{n=0}^{N-1} y_n^{'*}e^{-j\frac{2\pi}{N}nk}, k = 0, ..., N-1$, becomes,

$$Y_k^{'} = \sum_{l=0}^{N-1}\sqrt{P_0}X_l H_{N-l}^{'*}V_{l-k} + Z_k^{'*}, \quad k = 0, \ldots, N-1. \quad (6)$$

Where V_{l-k} is the complex weighting function of the conjugate path, given by

$$V_{l-k} = \frac{1}{N}\sum_{n=0}^{N-1} e^{j\frac{2\pi}{N}n(l-k-\Delta fT)}. \quad (7)$$

Note that FFT($h_n^{'*}$) is equal to $H_{N-l}^{'*}$. When the frequency offset to subcarrier spacing ratio is less than 5%, the property of the complex-conjugate cancellation with the complex weighting function is expressed as follows [11],

$$U_{l-k} + V_{l-k} \approx \begin{cases} 2, & \text{if } l = \text{k} \\ 0, & \text{if } l \neq \text{k} \end{cases}. \quad (8)$$

3. THE PROPOSED ZERO-PADDED COMPLEX CONJUGATE TECHNIQUE IN MIMO-OFDM SYSTEMS

3.1 System Model for Zero-Padded Complex Conjugate Cancellation Scheme

In this subsection, the proposed zero-padded complex-conjugate cancellation scheme in multiple-antenna systems is described as shown in Figure 2 [15]. The frequency-domain modulated symbols, X_l ($l = 0, ..., N-1$), will be firstly encoded with the zero-padded space-frequency coding block. The frequency-domain transmitted symbols, $D_{1,l}$ ($D_{1,l} = X_0, 0, X_1, 0, ..., X_{N/2-2}, 0, X_{N/2-1}, 0$, for $l = 0, ..., N-1$, respectively) and $D_{2,l}$ ($D_{2,l} = 0, X_1, 0, X_0, ..., 0, X_{N/2-1}, 0, X_{N/2-2}$, for $l = 0, ..., N-1$, respectively), are then transmitted through the first and the second antennas, respectively. The time-domain received signal of a primary path is shown below

$$y_n = (\sqrt{P_1}d_{1,n} \otimes h_{1,n} + \sqrt{P_2}d_{2,n} \otimes h_{2,n})e^{j\frac{2\pi}{N}n\Delta fT} + z_n, \quad (9)$$

and the complex-conjugate path is,

$$y_n^{'} = (\sqrt{P_1}d_{1,n}^* \otimes h_{1,n}^{'} + \sqrt{P_2}d_{2,n}^* \otimes h_{2,n}^{'})e^{j\frac{2\pi}{N}n\Delta fT} + z_n^{'}, \quad (10)$$

where P_1 and P_2 are the transmit power for the first and the second transmit antennas, respectively. Note that the frequency offset is fixed over the two-path time interval. Then, the frequency-domain received signal of a primary path can be expressed as follows,

$$\begin{aligned} Y_k &= \sum_{l=0}^{N-1}\sqrt{P_1}D_{1,l}H_{1,l}U_{l-k} \\ &\quad + \sum_{l=0}^{N-1}\sqrt{P_2}D_{2,l}H_{2,l}U_{l-k} + Z_k, \end{aligned} \quad (11)$$

and the frequency-domain received signal of a conjugate path can be expressed as follows,

$$\begin{aligned} Y_k^{'} &= \sum_{l=0}^{N-1}\sqrt{P_1}D_{1,l}H_{1,N-l}^{'*}V_{l-k} \\ &\quad + \sum_{l=0}^{N-1}\sqrt{P_2}D_{2,l}H_{2,N-l}^{'*}V_{l-k} + Z_k^{'*}. \end{aligned} \quad (12)$$

3.2 Received Signal Model for Four Consecutive Subcarriers

In this subsection, the received signals of four consecutive subcarriers will be described as follows. At the transmitter, the frequency-domain modulated symbols are encoded and arranged into a block of four subcarriers corresponding to the proposed zero-padded coding structure. As a result, the modulated symbols are rearranged over space-frequency allocation and then transmitted over two-transmit antenna, which can be expressed by

$$\vec{X}_{MIMO} = \begin{bmatrix} X_0 & 0 \\ 0 & X_1 \\ X_1 & 0 \\ 0 & X_0 \end{bmatrix}.$$

Note that the first and the second columns of $\vec{X}_{MIMO}$ correspond to the first and the second antennas, respectively, while the rows represent the order of subcarriers. At the receiver, the received signals of a primary path of four consecutive subcarriers can be written as

$$\begin{aligned} Y_0 &= \sqrt{P_1}X_0H_{1,0}U_0 + \sum_{l=1}^{\frac{N}{2}-1}\sqrt{P_1}X_lH_{1,2l}U_{2l} \\ &\quad + \sum_{l=1,3,\ldots}^{\frac{N}{2}-1}\sqrt{P_2}X_{l-1}H_{2,2l+1}U_{2l+1} \\ &\quad + \sum_{l=0,2,\ldots}^{\frac{N}{2}-1}\sqrt{P_2}X_{l+1}H_{2,2l+1}U_{2l+1} + Z_0, \end{aligned} \quad (13)$$

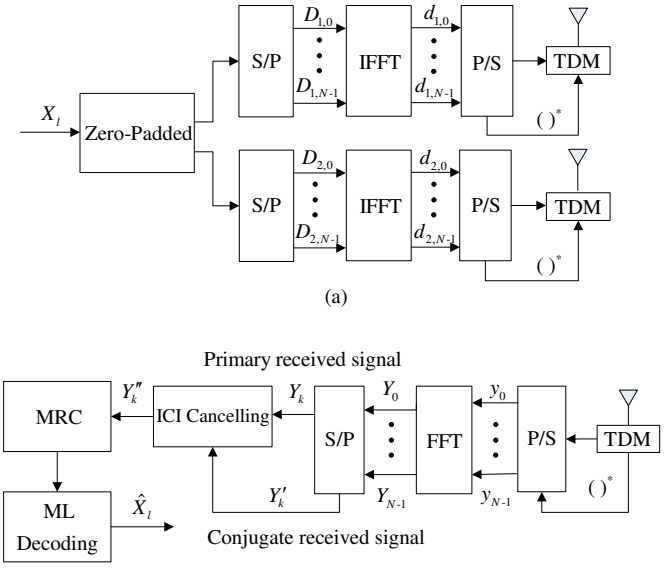

Fig.2: *Structure of a zero-padded complex conjugate cancellation scheme in MIMO-OFDM systems as (a) transmitter and (b) as receiver [15]*

$$Y_1 = \sqrt{P_2}X_1H_{2,1}U_0 + \sum_{l=0}^{\frac{N}{2}-1}\sqrt{P_1}X_lH_{1,2l}U_{2l-1} + \sum_{l=1,3,\ldots}^{\frac{N}{2}-1}\sqrt{P_2}X_{l-1}H_{2,2l+1}U_{2l} + \sum_{l=2,4,\ldots}^{\frac{N}{2}-1}\sqrt{P_2}X_{l+1}H_{2,2l+1}U_{2l} + Z_1, \quad (14)$$

$$Y_2 = \sqrt{P_1}X_1H_{1,2}U_0 + \sum_{l=0,l\neq 1}^{\frac{N}{2}-1}\sqrt{P_1}X_lH_{1,2l}U_{2l-2} + \sum_{l=1,3,\ldots}^{\frac{N}{2}-1}\sqrt{P_2}X_{l-1}H_{2,2l+1}U_{2l-1} + \sum_{l=0,2,\ldots}^{\frac{N}{2}-1}\sqrt{P_2}X_{l+1}H_{2,2l+1}U_{2l-1} + Z_2, \quad (15)$$

$$Y_3 = \sqrt{P_2}X_0H_{2,3}U_0 + \sum_{l=0}^{\frac{N}{2}-1}\sqrt{P_1}X_lH_{1,2l}U_{2l-3} + \sum_{l=1,3,\ldots}^{\frac{N}{2}-1}\sqrt{P_2}X_lH_{2,2l-1}U_{2l-4} + \sum_{l=2,4,\ldots}^{\frac{N}{2}-1}\sqrt{P_2}X_lH_{2,2l+3}U_{2l} + Z_3. \quad (16)$$

Similarly, the received signals of a complex-conjugate path are described as,

$$Y_0^{'} = \sqrt{P_1}X_0H_{1,N}^{'*}V_0 + \sum_{l=1}^{\frac{N}{2}-1}\sqrt{P_1}X_lH_{1,N-2l}^{'*}V_{2l} + \sum_{l=1,3,\ldots}^{\frac{N}{2}-1}\sqrt{P_2}X_{l-1}H_{2,N-(2l+1)}^{'*}V_{2l+1} + \sum_{l=0,2,\ldots}^{\frac{N}{2}-1}\sqrt{P_2}X_{l+1}H_{2,N-(2l+1)}^{'*}V_{2l+1} + Z_0^{'*}, \quad (17)$$

$$Y_1^{'} = \sqrt{P_2}X_1H_{2,N-1}^{'*}V_0 + \sum_{l=0}^{\frac{N}{2}-1}\sqrt{P_1}X_lH_{1,N-2l}^{'*}V_{2l-1} + \sum_{l=1,3,\ldots}^{\frac{N}{2}-1}\sqrt{P_2}X_{l-1}H_{2,N-(2l+1)}^{'*}V_{2l} + \sum_{l=2,4,\ldots}^{\frac{N}{2}-1}\sqrt{P_2}X_{l+1}H_{2,N-(2l+1)}^{'*}V_{2l} + Z_1^{'*}, \quad (18)$$

$$Y_2^{'} = \sqrt{P_1}X_1H_{1,N-2}^{'*}V_0 + \sum_{l=0,l\neq 1}^{\frac{N}{2}-1}\sqrt{P_1}X_lH_{1,N-2l}^{'*} V_{2l-2} + \sum_{l=1,3,\ldots}^{\frac{N}{2}-1}\sqrt{P_2}X_{l-1}H_{2,N-(2l+1)}^{'*}V_{2l-1} + \sum_{l=0,2,\ldots}^{\frac{N}{2}-1}\sqrt{P_2}X_{l+1}H_{2,N-(2l+1)}^{'*}V_{2l-1} + Z_2^{'*}, \quad (19)$$

$$Y_3^{'} = \sqrt{P_2}X_0H_{2,N-3}^{'*}V_0 + \sum_{l=0}^{\frac{N}{2}-1}\sqrt{P_1}X_lH_{1,N-2l}^{'*} V_{2l-3} + \sum_{l=1,3,\ldots}^{\frac{N}{2}-1}\sqrt{P_2}X_lH_{2,N-(2l-1)}^{'*}V_{2l-4} + \sum_{l=2,4,\ldots}^{\frac{N}{2}-1}\sqrt{P_2}X_lH_{2,N-(2l+3)}^{'*}V_{2l} + Z_3^{'*}. \quad (20)$$

Let us consider the (13)-(16) and (17)-(20), respectively, the first terms on the right hand side of them are the desired transmitted symbols while the second, third and fourth terms are the ICI generated by other subcarriers, represented as I_0, I_1, I_2, I_3 and $I_0^{'}, I_1^{'}, I_2^{'}, I_3^{'}$, respectively. The last terms are the AWGN.

3.3 ICI Cancellation and Frequency Diversity Combining Technique

In the proposed zero-padded complex-conjugate cancellation for MIMO-OFDM systems, the ICI cancellation technique is proposed to exploit the frequency diversity, especially in frequency-selective fading channels. Thanks to the transmitted symbols of the complex-conjugate scheme mapped onto the channel response of H_l and H_{N-l}, they may not suffer from fading simultaneously. The combined received signals can be expressed as

$$Y_0^{''} = H_{1,0}^{*}Y_0 + H_{1,N}^{'}Y_0^{'}, \quad (21)$$

$$Y_1^{''} = H_{2,1}^{*}Y_1 + H_{2,N-1}^{'}Y_1^{'}, \quad (22)$$

$$Y_2^{''} = H_{1,2}^{*}Y_2 + H_{1,N-2}^{'}Y_2^{'}, \quad (23)$$

$$Y_3^{''} = H_{2,3}^{*}Y_3 + H_{2,N-3}^{'}Y_3^{'}. \quad (24)$$

When the frequency offset is smaller than 5%, one could show that

$$U_0 = \frac{1}{N}\sum_{n=0}^{N-1} e^{j\frac{2\pi}{N}n\Delta fT} \approx 1, \quad (25)$$

and

$$V_0 = \frac{1}{N}\sum_{n=0}^{N-1} e^{-j\frac{2\pi}{N}n\Delta fT} \approx 1. \quad (26)$$

Substituting (13)-(16) and (17)-(20) in (21)-(24), the combined received signals then become

$$Y_0^{''} = \sqrt{P_1}(|H_{1,0}|^2 + |H_{1,N}^{'}|^2)X_0 + H_{1,0}^{*}(I_0 + Z_0) + H_{1,N}^{'}(I_0^{'} + Z_0^{'*}), \quad (27)$$

$$Y_1^{''} = \sqrt{P_2}(|H_{2,1}|^2 + |H_{2,N-1}^{'}|^2)X_1 + H_{2,1}^{*}(I_1 + Z_1) + H_{2,N-1}^{'}(I_1^{'} + Z_1^{'*}), \quad (28)$$

$$Y_2^{''} = \sqrt{P_1}(|H_{1,2}|^2 + |H_{1,N-2}^{'}|^2)X_1 + H_{1,2}^{*}(I_2 + Z_2) + H_{1,N-2}^{'}(I_2^{'} + Z_2^{'*}), \quad (29)$$

$$Y_3^{''} = \sqrt{P_2}(|H_{2,3}|^2 + |H_{2,N-3}^{'}|^2)X_0 + H_{2,3}^{*}(I_3 + Z_3) + H_{2,N-3}^{'}(I_3^{'} + Z_3^{'*}). \quad (30)$$

When the frequency-domain channel impulse response is approximately constant over these subcarriers and over two-path transmission, i.e. quasi-static fading channels, with the property of complex conjugate cancellation in (8), the ICI is very small compared with the noise. Hence, the ICI, i.e. $I_0, I_0^{'}, I_1, I_1^{'}, I_2, I_2^{'}, I_3$, and $I_3^{'}$, could be ignored (See Section 4.1). The combined received signal of the four consecutive subcarriers could be approximated as,

$$Y_0^{''} = 2\sqrt{P_1}|H_1|^2X_0 + H_1^{*}Z_0 + H_1Z_0^{'*}, \quad (31)$$

$$Y_1^{''} = 2\sqrt{P_2}|H_2|^2X_1 + H_2^{*}Z_1 + H_2Z_1^{'*}, \quad (32)$$

$$Y_2^{''} = 2\sqrt{P_1}|H_1|^2X_1 + H_1^{*}Z_2 + H_1Z_2^{'*}, \quad (33)$$

$$Y_3^{''} = 2\sqrt{P_2}|H_2|^2X_0 + H_2^{*}Z_3 + H_2Z_3^{'*}. \quad (34)$$

3.4 Space Diversity Combining Technique

In this subsection, when the transmit or receive antennas are equipped with sufficient spacing, the channel impulse response between antennas fades independently. The authors then combine a pair of received signals which is transmitted from two-transmit antenna corresponding to the zero-padded coding structure. To exploit the space diversity, a pair of received signals (31) and (34), and (32) and (33), respectively, will be combined by using the maximal ratio combin-

ing [17], which can be expressed as,

$$\tilde{X}_0 = a_0 Y_0^{''} + a_3 Y_3^{''}, \quad (35)$$

$$\tilde{X}_1 = a_1 Y_1^{''} + a_2 Y_2^{''}. \quad (36)$$

Assuming that the transmitted symbols have a unit average energy. To find the coefficient a_0, a_1, a_2, and a_3, it is obvious that the optimum value of a_1 and a_2 should be determined such that the SNR of (36) will be maximized. By using the Schwarz inequality [17], these coefficients are equal to $a_1 = \frac{\sqrt{P_2}}{N_0}$ and $a_2 = \frac{\sqrt{P_1}}{N_0}$, and similarly, in (35), a_0 and a_3 can be also determined as $a_0 = \frac{\sqrt{P_1}}{N_0}$ and $a_3 = \frac{\sqrt{P_2}}{N_0}$. Next, the maximum-likelihood (ML) detector is employed for detecting the transmitted symbols.

4. PERFORMANCE ANALYSIS

In this section, the outage probability for the zero-padded complex conjugate cancellation scheme in MIMO-OFDM systems is investigated. For a fair comparison with the conventional complex-conjugate cancellation scheme, the outage probability of repetition-coded complex conjugate cancellation in SISO-OFDM systems is also investigated, given that the total transmit power and the code rate are the same. An outage occurs when a signal-to-noise ratio (SNR) of the systems falls below a predefined threshold, γ_{th}. From the experimental result, the neighboring subcarrier, i.e. the closest subcarrier on the left and right hand sides, will predominantly generate ICI to the specific subcarrier. Hence, the authors could simplify the problem, without loss of generality, by only considering the adjacent subcarrier and ignoring the rest of the subcarriers. Assuming that the frequency-domain channel impulse response is approximately constant over these subcarriers and over two-path transmission, i.e. Rayleigh quasi-static fading channels, with the property in (8), the ICI approaches to zero in the presence of small frequency offsets. In addition, these cases can be considered as noise limited system in which an outage can be caused by deep fades when the instantaneous SNR γ is driven below γ_{th}, namely

$$P_{Out} = P[\gamma < \gamma_{th}] = 1 - \int_{\gamma_{th}}^{\infty} f_{\Gamma}(\gamma)\, d\gamma. \quad (37)$$

4.1 Outage Probability for Zero-Padded Complex Conjugate Cancellation in MIMO-OFDM Systems

For the sake of simplicity, let us consider the transmitted symbol X_1 in $\vec{X}_{MIMO}$. Then, the received signal of transmitted symbol X_1 on the 1^{st} receiving subcarrier for the primary path in MIMO-OFDM systems can be expressed as,

$$Y_1 = \sqrt{P_2} H_2 X_1 U_0 + \sqrt{P_1} H_1 (X_0 U_{-1} + X_1 U_1) + Z_1, \quad (38)$$

and for the complex-conjugate path, it is

$$Y_1^{'} = \sqrt{P_2} H_2^{*} X_1 V_0 + \sqrt{P_1} H_1^{*} (X_0 V_{-1} + X_1 V_1) + Z_1^{'*}. \quad (39)$$

The combined received signal between Y_1 and $Y_1^{'}$ on the 1^{st} receiving subcarrier can be described as,

$$\begin{aligned} Y_1^{''} &= \frac{1}{N_0}(\sqrt{P_2} H_2^{*} Y_1 + \sqrt{P_2} H_2 Y_1^{'}), \\ &= \frac{P_2 |H_2|^2 X_1 (U_0 + V_0)}{N_0} + \frac{\sqrt{P_1 P_2}}{N_0}[X_0 (H_2^{*} H_1 \\ &\quad U_{-1} + H_2 H_1^{*} V_{-1}) + X_1 (H_2^{*} H_1 U_1 + H_2 H_1^{*} \\ &\quad V_1)] + \frac{\sqrt{P_2}}{N_0}(H_2^{*} Z_1 + H_2 Z_1^{'*}). \end{aligned} \quad (40)$$

The terms on the right hand side of (40) is the desired

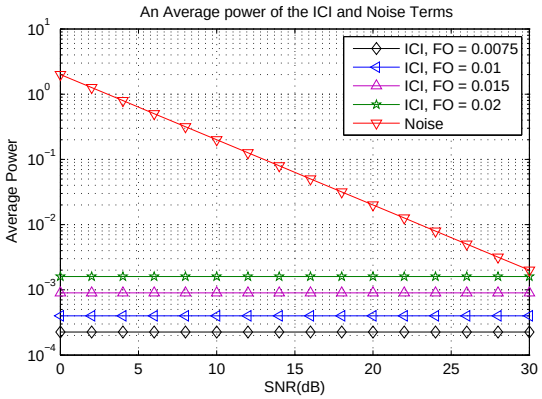

Fig.3: *The comparison of an average power of the ICI and noise terms*

transmitted symbol, the ICI, and noise, respectively. In order to compare the ICI with the noise, the average power of the ICI term and the noise term can be then expressed, respectively, as

$$P_1 P_2 \sigma_1^2 \sigma_2^2 (|U_{-1}|^2 + |V_{-1}|^2 + |U_1|^2 + |V_1|^2), \quad (41)$$

$$2 P_2 \sigma_2^2 N_0. \quad (42)$$

Note that σ_1^2 and σ_2^2 are the variances of channel H_1 and H_2, respectively, assuming that H_1 and H_2 are uncorrelated. From (41) and (42), let us assume that both P_1 and P_2 are set to 1 Watt, and both σ_1^2 and σ_2^2 are also set to 1. It is obviously seen that this ICI term is relatively small compared with the noise term when the frequency offset to subcarrier frequency spacing ratio is not greater than 2% corresponding to the maximum allowance in WiMax systems [18], as shown in Figure 3. Thus, this ICI term could be ignored in the following analysis for the sake of exposition. However, the authors will take this term into account in the simulations without loss of

generality. The combined received signal can be then approximated by

$$Y_1^{''} \approx \frac{2P_2|H_2|^2X_1}{N_0} + \frac{\sqrt{P_2}}{N_0}(H_2^*Z_1 + H_2Z_1^{'*}). \quad (43)$$

Similarly, it is straightforward to get the combined received signal between Y_2 and $Y_2^{'}$ on the 2^{nd} receiving subcarrier as follows,

$$\begin{aligned} Y_2^{''} &= \frac{1}{N_0}(\sqrt{P_1}H_1^*Y_2 + \sqrt{P_1}H_1Y_2^{'}), \\ &\approx \frac{2P_1|H_1|^2X_1}{N_0} + \frac{\sqrt{P_1}}{N_0}(H_1^*Z_2 + H_1Z_2^{'*}). \end{aligned} \quad (44)$$

Assuming that the transmitted symbols have unit average energy. The approximate signal-to-noise ratio (SNR) of the MRC output can be expressed as follows [17],

$$\gamma \approx \gamma_{Y_1^{''}} + \gamma_{Y_2^{''}}. \quad (45)$$

Thus, the approximated overall SNR of zero-padded complex conjugate cancellation scheme in MIMO-OFDM systems can be approximated by

$$\gamma \approx \frac{2}{N_0}(P_1|H_1|^2 + P_2|H_2|^2), \quad (46)$$

where H_1 and H_2 are modelled as two Gaussian random variables with zero mean and variance of $\sigma^2/2$ with the signal envelop of Rayleigh-distribution. Since $|H|^2$ is exponential distributed with mean of σ^2, then PDF of γ can be derived by finding the Jacobian of transformation and using transformation of two random variables. The PDF for the case of equal channel variances ($\lambda_1 = \lambda_2 = \lambda_0; \lambda_i = 1/\sigma_i^2$) and equal transmit powers ($P_1 = P_2 = P_0$) can be expressed as,

$$f_\Gamma(\gamma) = \frac{\lambda_0^2N_0^2\gamma}{4P_0^2}e^{-\lambda_0\frac{N_0}{2P_0}\gamma}, \quad (47)$$

and the PDF for the case of unequal channel variances ($\lambda_1 \neq \lambda_2$) can be described as,

$$f_\Gamma(\gamma) = \frac{\lambda_1\lambda_2N_0}{2(\lambda_1P_2 - \lambda_2P_1)}(e^{-\lambda_2\frac{N_0}{2P_2}\gamma} - e^{-\lambda_1\frac{N_0}{2P_1}\gamma}). \quad (48)$$

The outage probability of (47) for the case of equal channel variances can be expressed as,

$$P_{Out} = 1 - (\frac{\lambda_0N_0\gamma_{th}}{2P_0} + 1)e^{-\lambda_0\frac{N_0}{2P_0}\gamma_{th}}, \quad (49)$$

and the outage probability of (48) for the case of unequal channel variances can be described as,

$$\begin{aligned} P_{Out} &= 1 - (\frac{\lambda_2P_1e^{\lambda_2\frac{N_0}{2P_2}\gamma_{th}} - \lambda_1P_2e^{\lambda_1\frac{N_0}{2P_1}\gamma_{th}}}{\lambda_2P_1 - \lambda_1P_2}) \\ &\quad e^{-(\frac{\lambda_1P_2+\lambda_2P_1}{2P_1P_2})N_0\gamma_{th}}. \end{aligned} \quad (50)$$

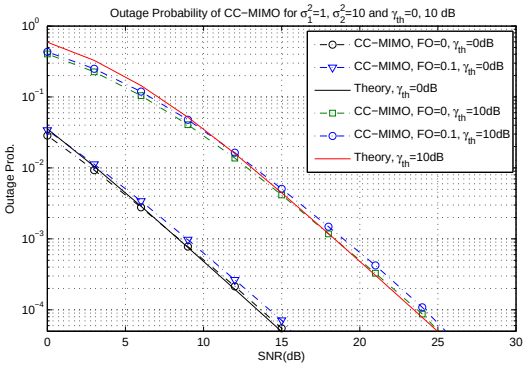

Fig.4: *The curves of outage probability versus SNR (dB) for zero-padded MIMO-OFDM conjugate cancellation*

To verify the derived outage probability expression in (50), the outage probability performance comparison between simulation and theoretical analysis of the zero-padded conjugate cancellation in MIMO-OFDM systems is shown in Figure 4. Note that both P_1 and P_2 are set to 0.5 Watts, and the frequency offset to subcarrier frequency spacing ratio is set to 0 and 0.1, respectively. In addition, a channel variance of H_1 and H_2 is set to 1 and 10, respectively. These curves show that the theoretical results perform close to the simulation results.

4.2 Outage Probability for Repetition-Coded Complex Conjugate Cancellation in OFDM Systems

For the sake of consistent comparison with the conventional complex-conjugate systems given the same code rate constraint, as shown in Figure 2, the modulated symbols of four consecutive subcarriers are transmitted with a repetition-coded structure expressed as,

$$\vec{X}_{SISO} = \begin{bmatrix} X_0 \\ X_1 \\ X_0 \\ X_1 \end{bmatrix}.$$

The outage performance for these systems is also investigated. Let us also consider the transmitted symbol X_1 in $\vec{X}_{SISO}$. Then, the received signal of transmitted symbol X_1 on the 1^{st} receiving subcarrier for the primary path in SISO-OFDM systems can be expressed as,

$$Y_1 = \sqrt{P_0}H(X_1U_0 + X_0U_{-1} + X_0U_1) + Z_1, \quad (51)$$

and for the complex-conjugate path, it is

$$Y_1^{'} = \sqrt{P_0}H^*(X_1V_0 + X_0V_{-1} + X_0V_1) + Z_1^{'*}. \quad (52)$$

The combined received signal between Y_1 and $Y_1^{'}$ on the 1^{st} receiving subcarrier can be described as,

$$\begin{aligned} Y_1^{''} &= \frac{1}{N_0}(\sqrt{P_0}H^*Y_1 + \sqrt{P_0}HY_1^{'}), \\ &\approx \frac{2P_0|H|^2X_1}{N_0} + \frac{\sqrt{P_0}}{N_0}(H^*Z_1 + HZ_1^{'*}) \quad (53) \end{aligned}$$

Similarly, it is straightforward to get the combined received signal between Y_3 and $Y_3^{'}$ on the 3^{rd} receiving subcarrier as follows,

$$\begin{aligned} Y_3^{''} &= \frac{1}{N_0}(\sqrt{P_0}H^*Y_3 + \sqrt{P_0}HY_3^{'}), \\ &\approx \frac{2P_0|H|^2X_1}{N_0} + \frac{\sqrt{P_0}}{N_0}(H^*Z_3 + HZ_3^{'*}) \quad (54) \end{aligned}$$

Note that the transmitted symbol is assumed to has unit average energy. Similarly, in (45), $\gamma \approx \gamma_{Y_1^{''}} + \gamma_{Y_3^{''}}$, the approximated overall SNR of repetition-coded complex conjugate cancellation in SISO-OFDM systems can be described by

$$\gamma = \frac{4P_0|H|^2}{N_0}. \quad (55)$$

Note that P_0 is the transmit power. The PDF of γ can also be derived by finding the Jacobian of transformation. Then, the PDF can be expressed as,

$$f_\Gamma(\gamma) = \frac{\lambda_0 N_0}{4P_0} e^{-\lambda_0 \frac{N_0}{4P_0}\gamma}. \quad (56)$$

The outage probability of (56) can be expressed as,

$$P_{Out} = P[\gamma < \gamma_{th}] = 1 - e^{-\lambda_0 \frac{N_0}{4P_0}\gamma_{th}}. \quad (57)$$

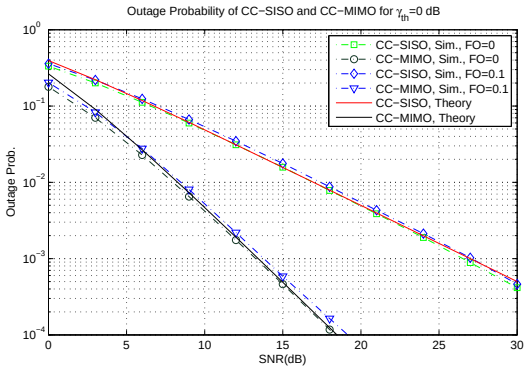

Fig.5: *The curves of outage probability versus SNR (dB) for complex conjugate cancellation in SISO and MIMO systems with γ_{th} of 0 dB*

Next, the derived outage probability expressions

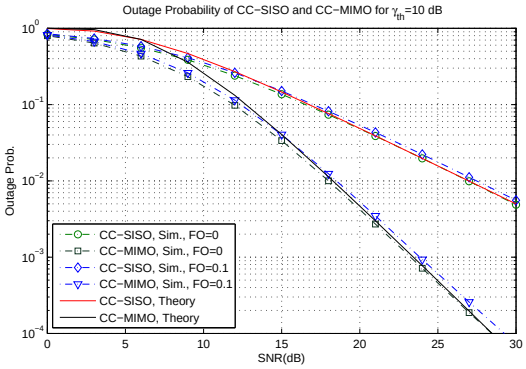

Fig.6: *The curves of outage probability versus SNR (dB) for complex conjugate cancellation in SISO and MIMO systems with γ_{th} of 10 dB*

in (49) for the proposed system and (57) for the conventional one will be investigated. Figures 5 and 6 show the comparison between the outage probability of zero-padded MIMO and repetition-coded SISO conjugate cancellation schemes in both theoretical and simulation aspects, in which γ_{th} is set to 0 dB and 10 dB, respectively; P_0, P_1, and P_2 are set to 0.5 Watts; and the variances of channel, σ_0^2, σ_1^2 ,and σ_2^2 are set to 1. Note that the first and second antennas are excited in different times for zero-padded MIMO-OFDM systems. The frequency offset to subcarrier frequency spacing ratio is set to 0 and 0.1, respectively. These curves also show that the theoretical results perform close to the simulation results. In addition, it is obviously seen that the diversity of MIMO systems is higher than the SISO systems.

5. SIMULATION RESULTS

In this section, the performance evaluation of the proposed zero-padded complex conjugate cancellation technique in MIMO-OFDM systems is examined in time-varying frequency-selective fading channels through a computer simulation. The transmitted power of the proposed system is half of the ordinary MIMO-OFDM systems for a fair comparison. The bandwidth efficiency is 1 bit/s/Hz. Since the proposed system and the repetition-coded conjugate cancellation scheme require four subcarriers and two TDM time slots to transmit two information symbols, the QPSK modulation is employed for both of them, while the ordinary one uses BPSK modulation. In addition, Jake's model [19] is employed with a normalized Doppler shift of 5,000 Hz and the six paths Typical Urban (TU) delay profile [20] for simulating both Rician ($K_{Line\ of\ Sight} = 1$) and Rayleigh fading channels. Note that the Doppler shift for the LOS is assumed to be zero. The ΔfT is investigated as 0.01, 0.1, and 0.2, respectively. The simulations assume that the perfect knowledge of the channels is known at the receiver. The total number of transmitted OFDM symbols is 100,000. Each OFDM symbol

utilizes $N = 64$ subcarriers.

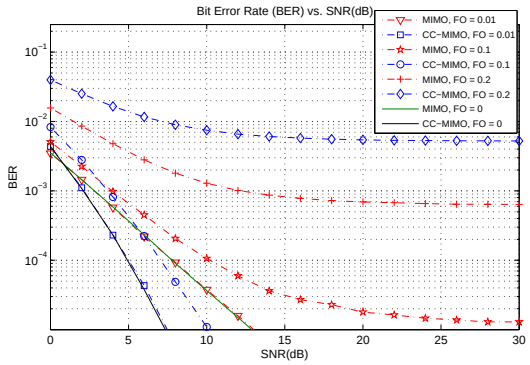

Fig.7: *The curves of BER versus SNR (dB) for Rician fading channels*

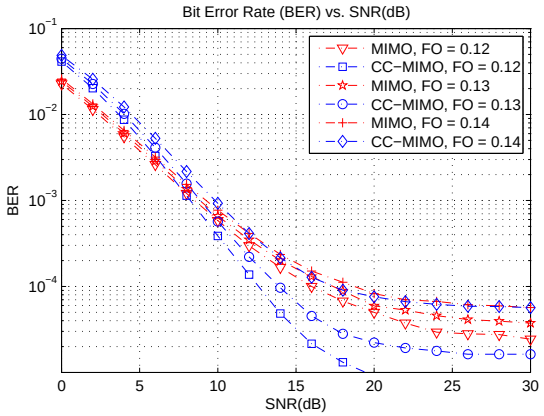

Fig.8: *The curves of BER versus SNR (dB) for Rayleigh fading channels, increasing FO*

Figure 7 presents the BER versus SNR (dB) for the proposed zero-padded complex conjugate cancellation in MIMO-OFDM systems and the ordinary zero-padded MIMO-OFDM systems, in Rician fading channels. It is worth noting that, at BER of 10^{-4} for ΔfT of 0.01 and 0.1, the proposed system has a SNR gain of 3 dB over the ordinary zero-padded MIMO-OFDM systems. It is conceivable that the proposed system offers more diversity gain than that of the ordinary one. This would be the benefit from transmitting complex conjugate path which could reduce the effect of ICI and obtain the frequency diversity gain. Moreover, when ΔfT is large ($\Delta fT = 0.2$), the BER performance of the ordinary zero-padded MIMO-OFDM systems is obviously better than that of the proposed system.

Figure 8 presents the BER versus SNR (dB) for the proposed system and the ordinary zero-padded MIMO-OFDM systems in Rayleigh fading channels by increasing ΔfT from 0.12 to 0.14. It is important to note that, at high SNR, the performance of the proposed system is better than that of the ordinary one when the frequency offset is less than 14% of sub-

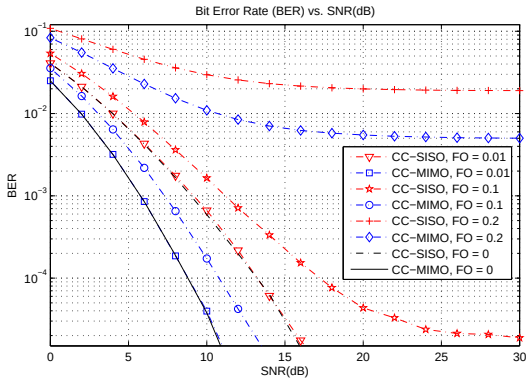

Fig.9: *The curves of BER versus SNR (dB) for complex conjugate cancellation in SISO and MIMO systems, in Rayleigh fading channels*

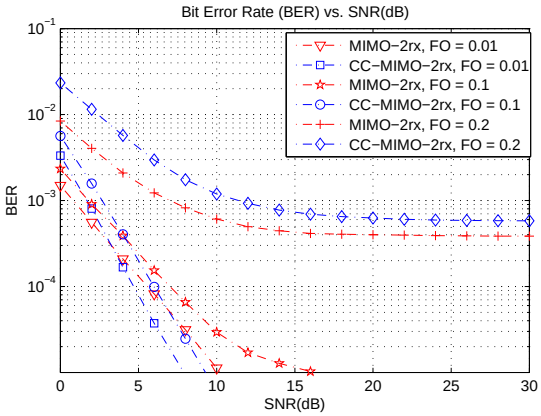

Fig.10: *The curves of BER versus SNR (dB) for Rayleigh fading channels, two-receive antenna*

carrier spacing. It is shown that the proposed system is robust to frequency offset situations.

Figure 9 presents the BER versus SNR (dB) for the proposed system and the repetition-coded complex conjugate cancellation in SISO-OFDM systems, in Rayleigh fading channels. It is worth noting that, if ΔfT is small such as 0.01 and 0.1, the proposed system is better than the repetition-coded complex conjugate cancellation technique in SISO-OFDM systems about the SNR gain of 5 dB at BER of 10^{-4} (when $\Delta fT = 0.01$) and about the SNR gain of 7 dB at BER of 10^{-4} (when $\Delta fT = 0.1$). Thanks to the multiple-antenna system and two-path complex-conjugate transmission, it is conceivable that the proposed system achieves higher diversity than that of the repetition-coded complex conjugate cancellation system because of using two-transmit antenna. Furthermore, if ΔfT is large ($\Delta fT = 0.2$), the BER performance of the proposed system is obviously better than that of the repetition-coded complex conjugate cancellation in SISO-OFDM systems.

Figure 10 presents the BER versus SNR (dB) for the proposed system and the ordinary zero-padded MIMO-OFDM systems for two receive antennas, in

Rayleigh fading channels. It is important to note that, when ΔfT is small ($\Delta fT = 0.01, 0.1$), the proposed scheme is better than the ordinary case about SNR gain of 1 dB at BER of 10^{-4}. It is conceivable that the performance gap between the proposed system and the ordinary one is quite small. Although this significant performance improvement of the ordinary one is attained by the space diversity in the two-received antenna system, the proposed system still performs better. In addition, when ΔfT is large ($\Delta fT = 0.2$), the BER of the ordinary zero-padded MIMO-OFDM systems is better than that of the proposed system.

6. CONCLUSIONS

In this paper, the zero-padded complex conjugate cancellation for ICI cancellation with diversity combining in MIMO-OFDM systems has been proposed. Simulation results show that when the frequency offset is less than 10%, the proposed system outperforms the ordinary zero-padded MIMO-OFDM systems with the SNR gain of 3 dB at BER of 10^{-4} is observed in Rician fading channels. In Rayleigh fading channels, the performance of the proposed system is almost identical to the ordinary one when the frequency offset is about 14%, at high SNR. In addition, the SNR gain of 1 dB could be attained at BER of 10^{-4} for two-receive antenna case. In comparison with the repetition-coded complex conjugate cancellation, the proposed system outperforms of about 5 dB at BER of 10^{-4}. Hence, the proposed system is useful for frequency offset situations in MIMO-OFDM systems. Moreover, the derived outage probability can be used as the performance approximation of the proposed system.

References

[1] A. Goldsmith, Wireless Communications, Cambridge University Press, 2005.

[2] D. Tse and P. Viswanath, Fundamentals of Wireless Communication, Cambridge University Press, 2005.

[3] J. Ahn and H.S. Lee, "Frequency domain equalization of OFDM signal over frequency nonselective Rayleigh fading channels," *IEEE Electronic Letters*, vol. 29, no. 16, pp. 1476-1477, 1993.

[4] C. Muschallik, "Improving an OFDM reception using an adaptive Nyquist windowing," *IEEE Transactions on Consumer Electronics*, vol. 42, pp. 259-269, 1996.

[5] Y. Zhao and S.-G. Haggman, "Intercarrier interference self-cancellation scheme for OFDM mobile communication systems," *IEEE Transactions on Communications*, vol. 49, no. 7 , pp. 1185-1191, 2001.

[6] J. Armstrong, "Analysis of new and existing methods of reducing intercarrier interference due to carrier frequency offset in OFDM," *IEEE Transactions on Communications*, vol. 47, no. 3 , pp. 365-369, 1999.

[7] K. Sathananthan, C. R. N. Athaudage and B. Qiu, "A novel ICI cancellation scheme to reduce both frequency offset and IQ imbalance effects in OFDM," *in Proceedings of the 9th International Symposium on Computers and Communications (ISCC'04)*, vol. 2, pp. 708-713, July 2004.

[8] S. Tang, K. Gong, J. Song, C. Pan and Z. Yang, "Intercarrier interference cancellation with frequency diversity for OFDM systems," *IEEE Transactions on Broadcasting*, vol. 53, no. 1, pp. 132-137, 2007.

[9] K.-H. Kim and B. Seo, "Efficient ICI self-cancellation scheme for OFDM systems," *ETRI Journal*, vol. 36, no. 4, pp. 537-544, 2014.

[10] H.-G. Yeh and Y.-K. Chang, "New parallel algorithm for mitigating the frequency offset of OFDM systems," *in Proceedings of the 60th IEEE Vehicular Technology Conference (VTC'04-Fall)*, Los Angeles, CA, pp. 2087-2091, Sep. 2004.

[11] H.-G. Yeh, Y.-K. Chang and B. Hassibi, "A Scheme for cancelling intercarrier interference using conjugate transmission in multicarrier communication systems," *IEEE Transactions on Wireless Communications*, vol. 6, no. 1, pp. 3-7, 2007.

[12] C.-L. Wang and Y.-C. Huang, "Intercarrier interference cancellation using general phase rotated conjugate transmission for OFDM," *IEEE Transactions on Communications*, vol. 58, pp. 812-819, 2010.

[13] D.-N. Dao and C. Tellambura, "Intercarrier interference self-cancellation space-frequency codes for MIMO-OFDM," *IEEE Transactions on Vehicular Technology*, vol. 54, no. 5, pp. 1729-1738, 2005.

[14] Z. Li and X.-G. Xia, "An alamouti coded OFDM transmission for cooperative systems robust to both timing errors and frequency offsets," *IEEE Transactions on Wireless Communications*, vol. 6, no. 1, pp. 1839-1844, 2007.

[15] A. Yiwleak and C. Pirak, "Zero-padded complex conjugate technique for intercarrier interference cancellation in MIMO-OFDM systems," *in Proceedings of International Symposium on Communications and Information Technologies (ISCIT'10)*, pp. 901-906, Oct. 2010.

[16] A. Yiwleak, C. Pirak and R. Mathar, "Zero-padded symmetric conjugate technique for intercarrier interference cancellation in MIMO-OFDM systems," *3rd International Congress on Ultra Modern Telecommunications and Control Systems and Workshops (ICUMT'11)*, pp. 1-6, Oct. 2011.

[17] D.G. Brennan, "Linear diversity combining techniques," *Proceedings of the IEEE*, vol. 91, no. 2,

pp. 331-356, 2003.

[18] IEEE Std 802.16e-2005 and IEEE Std 802.16-2004jCorl-2005, IEEE Standard for Local and Metropolitan Area Networks Part 16: Air Interface for Fixed and Mobile Broadband Wireless Access Systems Amendment 2: Physical and Medium Access Control Layers for Combined Fixed and Mobile Operation in Licensed Bands, New York: IEEE, Feb. 2006.

[19] J.G. Proakis, Digital Communications, McGraw-Hill, New York, 4th edition, 2000.

[20] Y.G. Li, N. Seshadri and S. Ariyavisitakul, "Channel estimation for OFDM systems with transmitter diversity in mobile wireless channels," *IEEE Journal on Selected Areas in Communications*, vol. 17, No. 3, pp. 461-471, 1999.

Aurupong Yiwleak received the Bachelor degree from Prince of Songkla University, Thailand, in 1996 and the Master degree from Asian Institute of Technology, Thailand, in 2005. Currently, he is a Ph.D. candidate in wireless communication engineering laboratory of The Sirindhorn International Thai-German Graduate School of Engineering (TGGS), King Mongkut's University of Technology North Bangkok, Thailand.

Chaiyod Pirak received the Bachelor degree in telecommunication engineering from King Mongkut's Institute of Technology Ladkrabang, Bangkok, Thailand in 2001 and the Ph.D. degree from University of Maryland, College Park, MD, USA in 2005. He is holding a lecturer position at communications engineering department of TGGS. His research interests include the area of wireless communications.